

RESEARCH

Open Access



Rhei Undulati Rhizoma attenuates memory decline and reduces amyloid- β induced neuritic dystrophy in 5xFAD mouse

Seungmin Lee¹, In Gyoung Ju², Hyeyoon Eo¹, Jin Hee Kim¹, Yujin Choi¹ and Myung Sook Oh^{1,2,3*} 

Abstract

Background Alzheimer's disease (AD) is a common type of dementia characterized by amyloid- β (A β) accumulation, lysosomal dysfunction, and tau hyperphosphorylation, leading to neurite dystrophy and memory loss. This study aimed to investigate whether Rhei Undulati Rhizoma (RUR), which has been reported to have anti-neuroinflammatory effect, attenuates A β -induced memory impairment, neuritic dystrophy, and tau hyperphosphorylation, and to reveal its mode of action.

Methods Five-month-old 5xFAD mice received RUR (50 mg/kg) orally for 2 months. The Y-maze test was used to assess working memory. After behavioral testing, brain tissue was analyzed using thioflavin S staining, western blotting, and immunofluorescence staining to investigate the mode of action of RUR. To confirm whether RUR directly reduces A β aggregation, a thioflavin T assay and dot blot were performed after incubating A β with RUR.

Results RUR administration attenuated the A β -induced memory impairment in 5xFAD mice. Furthermore, decreased accumulation of A β was observed in the hippocampus of the RUR-treated 5xFAD group compare to the vehicle-treated 5xFAD group. Moreover, RUR reduced the dystrophic neurites (DNs) that accumulate impaired endolysosomal organelles around A β . In particular, RUR treatment downregulated the expression of β -site amyloid precursor protein cleaving enzyme 1 and the hyperphosphorylation of tau within DN. Additionally, RUR directly suppressed the aggregation of A β , and eliminated A β oligomers in vitro.

Conclusions This study showed that RUR could attenuate A β -induced pathology and directly regulate the aggregation of A β . These results suggest that RUR could be an efficient material for AD treatment through A β regulation.

Keywords Rhei Undulati Rhizoma, Amyloid- β , Dystrophic neurites, β -Site amyloid precursor protein cleaving enzyme-1, Tau hyperphosphorylation

*Correspondence:

Myung Sook Oh
msohok@khu.ac.kr

Full list of author information is available at the end of the article



© The Author(s) 2024. **Open Access** This article is licensed under a Creative Commons Attribution 4.0 International License, which permits use, sharing, adaptation, distribution and reproduction in any medium or format, as long as you give appropriate credit to the original author(s) and the source, provide a link to the Creative Commons licence, and indicate if changes were made. The images or other third party material in this article are included in the article's Creative Commons licence, unless indicated otherwise in a credit line to the material. If material is not included in the article's Creative Commons licence and your intended use is not permitted by statutory regulation or exceeds the permitted use, you will need to obtain permission directly from the copyright holder. To view a copy of this licence, visit <http://creativecommons.org/licenses/by/4.0/>. The Creative Commons Public Domain Dedication waiver (<http://creativecommons.org/publicdomain/zero/1.0/>) applies to the data made available in this article, unless otherwise stated in a credit line to the data.

Based on previous reports, we hypothesized that RUR attenuates AD pathology.

In this study, we evaluated the effect of RUR on the pathological characteristics of AD in the 5xFAD mouse. We administered RUR orally to 5xFAD transgenic mice and performed a behavior test to investigate the effect of RUR on A β -induced memory loss. Furthermore, we measured the effects of RUR on A β accumulation, neuritic dystrophy, and tau hyperphosphorylation in the hippocampus of the brain of 5xFAD mice. Furthermore, we performed a thioflavin T (Th T) fluorescence assay to evaluate the anti-aggregation effect of RUR on β -sheet rich forms of A β .

Materials and methods

Materials

Horseradish peroxidase (HRP) conjugated mouse anti- β -actin antibody was purchased from Santa Cruz Biotechnology (Temecula, CA, USA). Rabbit anti-glyceraldehyde-3-phosphate dehydrogenase (GAPDH) antibody, rabbit anti-Protein kinase B (Akt) antibody, rabbit anti-phospho-Akt (serine 473) antibody, rabbit anti-Glycogen synthase kinase-3 (GSK-3 β) antibody, rabbit anti-phospho-GSK-3 β (serine 9), and rabbit anti-lysosomal-associated membrane protein 1 (LAMP1) antibody were purchased from Cell Signaling Technology (Danvers, MA, USA). Mouse anti- β -Amyloid antibody (6E10) was purchased from BioLegend (San Diego, CA, USA). A β ₁₋₄₂ peptide was purchased from AnaSpec (Fremont, CA, USA). Skim milk was purchased from BD Transduction Laboratories (Franklin Lakes, NJ, USA). Mouse anti-BACE1 antibody and polyvinylidene difluoride (PVDF) was purchased from Millipore (Burlington, MA, USA). Normal horse serum and anti-fade fluorescent mounting medium containing 4',6-diamidino-2-phenylindole were purchased from Vector Laboratories (Burlingame, CA, USA). Anti-mouse and anti-rabbit HRP secondary antibodies were purchased from Enzo Life Sciences, Inc. (Farmingdale, NY, USA). Tetramethylethylenediamine, protein assay reagent, acrylamide, enhanced chemiluminescence (ECL) reagent, protein standards dual color, and Tween 20 were purchased from Bio-Rad Laboratories (Hercules, CA, USA). Rabbit anti-CTF antibody, mouse anti-AT8 (phosphor-tau, serine 202/threonine 205) antibody, rabbit anti-oligomer antibody (A11), goat anti-rabbit Alexa 488, goat anti-mouse Alexa 594, and protease/phosphatase inhibitor cocktail were purchased from Thermo Fisher Scientific (Waltham, MA, USA). Nordihydroguaiaretic acid (NDGA), Th T, thioflavin S (Th S), and all the other reagents were purchased from Sigma-Aldrich (St. Louis, MO, USA), unless otherwise noted.

Preparation of RUR extract

RUR was purchased from the Kwangmyoungdang Medicinal Herbs (Naemomedah, Ulsan, Republic of Korea). RUR, the voucher specimen (BON19012401), was deposited in the herbarium of the College of Pharmacy at Kyung Hee University (Seoul, Republic of Korea). The dried rhizomes were extracted with 70% ethanol on rocking shaker for 24 h at room temperature. The extract was then filtered and lyophilized to obtain a powder (yield: 28.50%). The extract was resuspended in an appropriate vehicle before use. Extract of RUR was standardized the contents of rhapontin and rhapontigenin, the principal compounds of RUR that are known to suppress neuroinflammation and attenuate A β /tau-related AD pathological features, using an ultra performance liquid chromatography-photodiode array analysis [19, 23]

Animals and administration

We purchased 5xFAD (B6SJL-Tg(APP^{Sw}FLon, PSEN1^{M146L}*L286V)6799Vas/Mmjax) mouse from the Jackson Laboratory (Bar Harbor, ME, USA). 5xFAD mutations include APP KM670/671NL (Swedish), APP I716V (Florida), APP V717I (London), PSEN1 M146L, and PSEN1 L286V, resulting in early and aggressive A β accumulation related to memory deficits [24]. Five-month-old male and female wild-type (WT) and 5xFAD mouse were used in the experiments. Mouse were divided into three groups: WT (n=21), 5xFAD (n=11), and 5xFAD+RUR at 50 mg/kg (n=11). RUR at 50 mg/kg was dissolved in 2% tween 80 and orally administered using a Zonde needle to 5xFAD mouse for 2 months. The mouse were housed in plastic cages with constant temperature (23 \pm 1 $^{\circ}$ C), humidity (50 \pm 10%), and a 12 h light/dark cycle and free access to food and water. In this study, all animal studies were performed in accordance with the 'Guide for the Care and Use of Laboratory Animals, 8th edition' (National Institutes of Health, 2011).

Y-maze test

The Y-maze test was performed using a Y-shaped maze consisting of three arms (40 cm \times 3 cm \times 12 cm walls) to assess working memory [25]. The mouse was placed in the center of the Y-maze and allowed to explore each arm labeled A, B, or C. Arm entries and sequences were recorded for 8 min. Alternation behavior was defined as consecutive entries in three different arms without repetition: ABC, BCA, or CBA. The percentage of spontaneous alternations was calculated using the following equations: (number of alternations/total number of arm entries - 2) \times 100.

Brain tissue preparation

For tissue analysis, the mice were anesthetized and transcardially perfused with 0.05 M phosphate-buffered saline (PBS). After perfusion was complete, the mouse was fixed with 4% para-formaldehyde in 0.1 M phosphate buffer. The dissected brains were then post-fixed overnight at 4 °C, and immersed in 30% sucrose dissolved in PBS for cryoprotection. Serial 25 µm thick coronal sections were cut on a freezing sliding microtome (Leica Microsystems Inc., Nussloch, Germany) and stored in a cryoprotectant (25% ethylene glycol, 25% glycerol, and 0.05 M phosphate buffer) at 4 °C until use.

Thioflavin S (Th S) staining

For staining Aβ plaques, we used Th S, which interacts with the β-sheet structure of amyloid plaques and commonly visualizes the region of Aβ plaques in the mouse brain [26]. The free-floating sections were washed with PBS and mounted on adhesion microscope slides. The slides were incubated in the dark with 0.5% Th S for 20 min, rinsed with 50%, 70%, 90%, and 100% ethanol for 2 min each, and covered with mounting medium.

Immunofluorescence staining

For immunofluorescence staining, free-floating sections of mouse brains were rinsed in PBS and incubated for 1 h in a blocking solution containing 3% normal goat or horse serum, 2% bovine serum albumin, and 0.3% Triton X-100 at RT. After the blocking step, the sections were incubated with primary antibodies overnight at 4 °C. For visualization, they were subsequently incubated with secondary antibody for 1 h at RT. The sections were mounted and the cover-slipped using an anti-fade mounting medium containing 4',6-diamidino-2-phenylindole. Fluorescent images were captured using a K1-Fluo confocal microscope (Nanoscope Systems, Daejeon, Republic of Korea).

Western blot

Western blot was performed as previously described [27]. The hippocampal regions of mouse brains were dissected in the vehicle-treated WT group, vehicle-treated 5xFAD group, and RUR-treated 5xFAD group. Then, the hippocampus was homogenized in radio-immunoprecipitation assay lysis buffer (RIPA) containing protease/phosphatase inhibitors. The protein amount of the sample buffer was equalized to 30 µg using the Bradford assay. Protein samples were separated by sodium dodecyl sulfate–polyacrylamide gel electrophoresis, and transferred to PVDF membranes. Next, the membranes were incubated with blocking solution containing 5% bovine serum albumin or skim milk in 0.1% Tween 20 in tris-buffered saline for 1 h at RT, and reacted with primary

antibodies overnight at 4 °C. After that, they were incubated with HRP-conjugated secondary antibodies for 1 h at RT. The immunoreactive bands on the membrane were detected by the ECL reagent and visualized using ChemiDocXRS+ imaging system (Bio-Rad Laboratories). The quantification of band intensity was performed using the ImageJ software (Bethesda, MD, USA).

Aβ enzyme-linked immunosorbent assay (ELISA)

Aβ₁₋₄₂ and Aβ₁₋₄₀ ELISA was performed using fluorescent-based kit (Invitrogen, Camarillo, CA, USA) and appropriate Aβ₁₋₄₂ and Aβ₁₋₄₀ standards based on the product guideline, respectively. To obtain soluble fraction, right half of hippocampus was homogenized in RIPA buffer containing protease/phosphatase inhibitor and incubated on ice for 2h. After centrifugation at 15,000 rpm for 20 min, the supernatant (RIPA fraction) was collected and used as soluble proteins. The pellets were subsequently dissolved in 70% formic acid and incubated on ice for 2 h. After centrifugation at 15,000 rpm for 20 min, the supernatant (formic acid fraction) was neutralized by Tris base buffer and used as insoluble proteins [28]. Protein concentrations of soluble and insoluble protein samples were determined using the Bradford protein assay and Lowry protein assay, respectively.

Th T assay

Th T is commonly used to measure Aβ fibril aggregation and enhanced fluorescence emission when bound to the β-sheet of Aβ fibrils [26]. Aβ₁₋₄₂ monomer (5 µL of 100 µM in dimethyl sulfoxide) was incubated with PBS or RUR (0.3, 3, or 30 µg/mL) for 48 h at 37 °C. Then, 150 µL of 5 µM Th T solution diluted with 50 mM glycine-sodium hydroxide at pH 8.5 was added and incubated for 30 min at RT. Th T fluorescence was measured at 520 nm with excitation at 470 nm by FLUOstar Omega multimode microplate reader (BMG LABTECH GmbH, Ortenberg, Germany).

Dot blot

The Aβ₁₋₄₂ monomer (25 µM in DMEM/F-12 1:1 mixture) was incubated with PBS or RUR (0.3, 3, or 30 µg/mL) for 24 h at 4 °C to measure the effect of RUR on Aβ₁₋₄₂ oligomerization. Furthermore, the Aβ₁₋₄₂ oligomer (25 µM in DMEM/F-12 1:1 Mixture) was incubated with PBS or RUR (0.3, 3, or 30 µg/mL) for 3 h at 4 °C to measure the effect of RUR on Aβ₁₋₄₂ oligomer degradation. Then, 2 µL of each sample was spotted on PVDF membranes. The membrane was reacted with primary antibodies overnight at 4 °C. The membranes were incubated with HRP-conjugated secondary antibodies for 1 h at RT. The immunoreactive bands on the membrane were detected using an ECL reagent and visualized using a

ChemiDocXRS + imaging system (Bio-Rad Laboratories). The quantification of the band intensity was performed using ImageJ software (Bethesda, MD, USA).

Statistical analysis

All statistical parameters were calculated using GraphPad Prism version 8.0 software (GraphPad Software, San Diego, CA, USA). Values were expressed as the mean \pm standard error of the mean, and analyzed using one-way analysis of variance (ANOVA), followed by Dunnett's post hoc test or an unpaired Student's *t*-test. Differences with a *p* value less than 0.05 were considered statistically significant.

Results

Effect of RUR administration on memory decline in the 5xFAD mouse

The 5xFAD mice, a transgenic mouse well known as an AD model, are characterized by increased A β accumulation in the brain. Furthermore, in this model, memory impairment caused by A β accumulation is observed [24]. To identify whether RUR alleviates memory loss in 5xFAD mice, we administered RUR to 5-month-old 5xFAD mice for 2 months and performed a Y-maze test to assess working memory [29]. The total number of entries did not differ between the groups. The 5xFAD group showed a significantly lower percentage of spontaneous alternation (%) than the WT group. However, treatment with 50 mg/kg RUR markedly increased the percentage of spontaneous alternations (Fig. 1). Additionally, we performed MWM to assess the effect of RUR on spatial memory [30]. On the 5th day of training, the vehicle-treated 5xFAD group showed slower escape latency than the vehicle-treated WT group. However, the RUR-treated 5xFAD group had exhibited faster escape latency compared to the vehicle-treated 5xFAD group. Moreover, the time spent in the target quadrant on the probe trial, was significantly reduced in the vehicle-treated 5xFAD group compared to the vehicle-treated WT group, whereas this level was elevated in the RUR-treated 5xFAD group (Supplementary Figure S1).

Effect of RUR on A β accumulation in the brain of the 5xFAD mouse

To determine whether RUR could suppress the accumulation of A β , we stained the deposition of A β within the hippocampus and cortex using Th S staining and immunohistochemical analysis using 6E10. In Th S staining, RUR markedly reduced β -sheet-rich amyloid plaques in the hippocampus (Fig. 2A, B). Furthermore, RUR-treated 5xFAD mice had a significant decrease in 6E10-positive A β protein levels compared to vehicle-treated 5xFAD mice (Fig. 2C, D). However, in the cortex, no differences

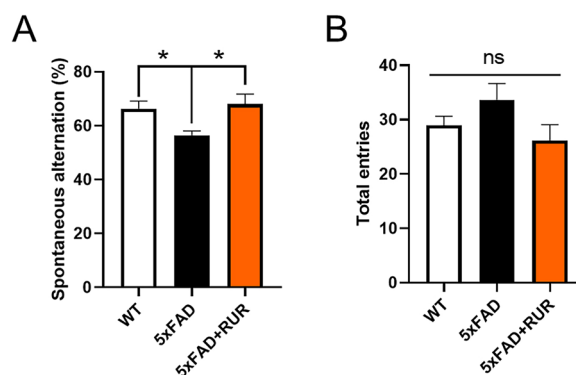


Fig. 1 Effects of Rhei Undulati Rhizoma (RUR) on memory decline in the 5xFAD mouse. Five-month-old WT and 5xFAD mice were administered vehicle or RUR (50 mg/kg) for 2 months. In the Y-maze test, spontaneous alternations (A) and total entries (B) were measured. The statistical analyses were performed using one-way analysis of variance (ANOVA), followed by Dunnett's post hoc test. **p* < 0.05 vs. 5xFAD group

were identified between the two groups in either assay. Moreover, we measured A β_{1-42} and A β_{1-40} levels in the hippocampus of 5xFAD mouse using ELISA kit. RUR administration reduced the soluble form of A β_{1-42} and A β_{1-40} levels and insoluble form of A β_{1-40} level in the hippocampus (Fig. 2E, F).

We also performed a western blot analysis to measure the protein expression levels of APP derivatives after cleavage. The protein level of soluble APP (sAPP) was higher in 5xFAD mice than in WT mice, while RUR remarkably downregulated the expression of the sAPP protein (Fig. 3A, B). Furthermore, we measured the CTF- β produced when APP is cleaved by β -secretase. We first measured the protein levels of CTF- β through western blotting. CTF- β protein was overexpressed in the vehicle-treated 5xFAD group compared to the vehicle-treated WT group. However, RUR treatment markedly reduced both fragments in a manner similar to that of sAPP (Fig. 3C, D).

Effect of RUR administration on the accumulation of DNs in the hippocampus of the 5xFAD mouse

To examine whether RUR could ameliorate the accumulation of DNs around the A β peptide, we co-stained with LAMP1 as the lysosomal marker, and 6E10 as the A β marker. The LAMP1-positive area was significantly larger in the vehicle-treated 5xFAD group than in the vehicle-treated WT group. In contrast, RUR treatment markedly reduced LAMP1 positive areas in the hippocampus (Fig. 4A, B). We also quantified the region of LAMP1 and 6E10 colocalization to assess whether RUR reduces the accumulated DNs around A β . We observed that RUR treatment reduced the co-stained regions of LAMP1 and

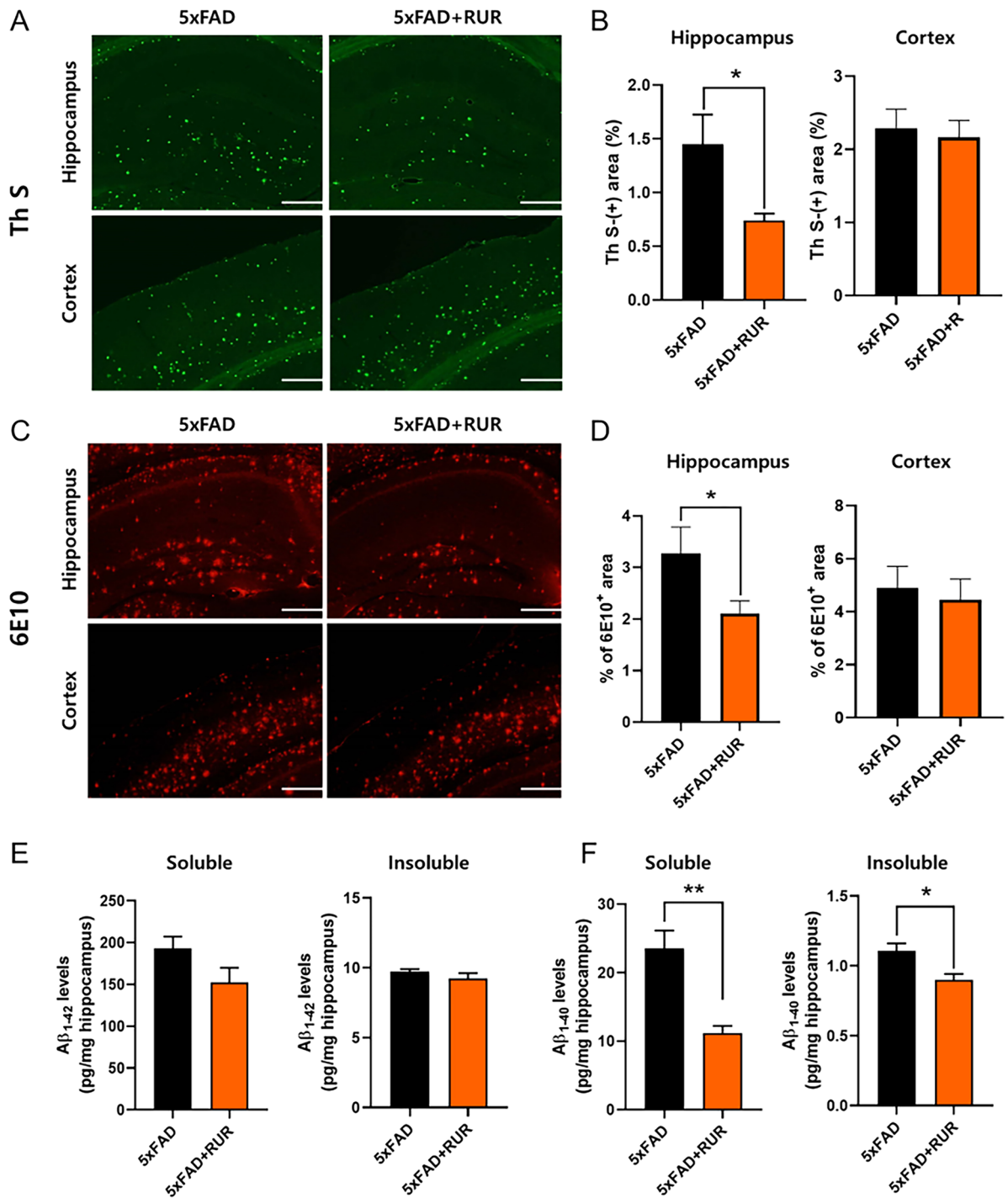


Fig. 2 Effect of RUR on Aβ accumulation in the brain of the 5xFAD mouse. Representative photomicrographs and quantifications for Th S staining (A, B) and 6E10 immunopositive areas (C, D) are shown in the hippocampus and cortex (n = 5–6 per group). Analysis of soluble and insoluble levels of Aβ₁₋₄₂ and Aβ₁₋₄₀ from the hippocampus of the mouse using ELISA kits (n = 5–6 per group). The statistical analyses were performed by unpaired Student's t test. **p* < 0.05 and ***p* < 0.01 vs. 5xFAD group. Scale bar = 200 μm. Aβ, amyloid-β; Th S, thioflavin S; 6E10, anti-Aβ antibody

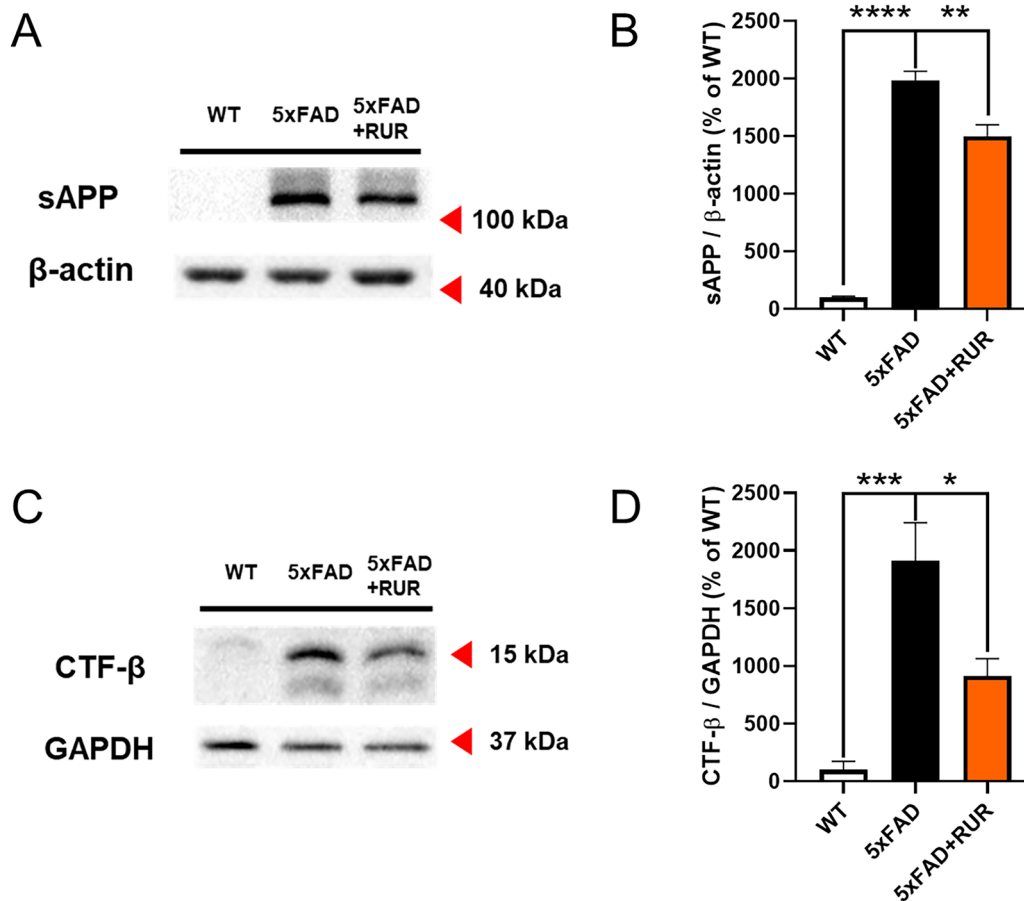


Fig. 3 Effect of RUR on derivatives of APP by cleavage in the hippocampus. The representative band image (A) and quantification (B) of sAPP are shown ($n=4-5$ per group). The protein level of sAPP was normalized to β -actin. The representative band image (C) and quantification (D) of CTF- β are shown ($n=4-5$ per group). The protein level of CTF- β was normalized to GAPDH. The statistical analyses were performed using ANOVA, followed by Dunnett's post hoc test. **** $p < 0.0001$, *** $p < 0.001$, ** $p < 0.01$, and * $p < 0.05$ vs. 5xFAD group. APP amyloid precursor protein, sAPP soluble APP, CTF- β c-terminal fragment - β , GAPDH glyceraldehyde-3-phosphate dehydrogenase

6E10, indicating that RUR treatment alleviated the accumulation of DNs (Fig. 4C).

Effect of RUR administration on the expression of BACE1 within DNs in the hippocampus of the 5xFAD mouse

To measure whether RUR could attenuate BACE1 accumulation within DNs around A β burden, we measured BACE1 levels within DNs using double immunofluorescence staining for LAMP1 and BACE1 in the hippocampus. The area co-stained with LAMP1 and BACE1 was larger in the vehicle-treated 5xFAD group than in the vehicle-treated WT group, while this area was significantly reduced in the RUR-treated 5xFAD group (Fig. 5A, B). BACE1 levels in the hippocampi of 5xFAD mice were measured by western blot analysis using anti-BACE1 antibody. The expression of BACE1 was significantly upregulated in the 5xFAD group compared to that in the WT group. Furthermore, 50 mg/kg RUR

markedly reduced BACE1 expression compared to the 5xFAD mouse group (Fig. 5C, D, Supplementary Figure S2).

Effect of RUR administration on the hyperphosphorylation of tau within DNs in the hippocampus of the 5xFAD mouse

To assess whether RUR alleviated tau phosphorylation within DNs, we co-stained hippocampal sections with LAMP1 and AT8 antibodies. The co-stained region of LAMP1 and AT8 increased markedly in the vehicle-treated 5xFAD group compared to the vehicle-treated WT group. However, this area was significantly reduced in the RUR-treated 5xFAD group compared to that in the vehicle-treated 5xFAD group (Fig. 6A, B). Phosphorylated levels of tau in the hippocampus were measured by western blot analysis using anti-AT8. Similarly to the results of immunofluorescence staining, the phosphorylated ratio of tau was increased in 5xFAD mice compared

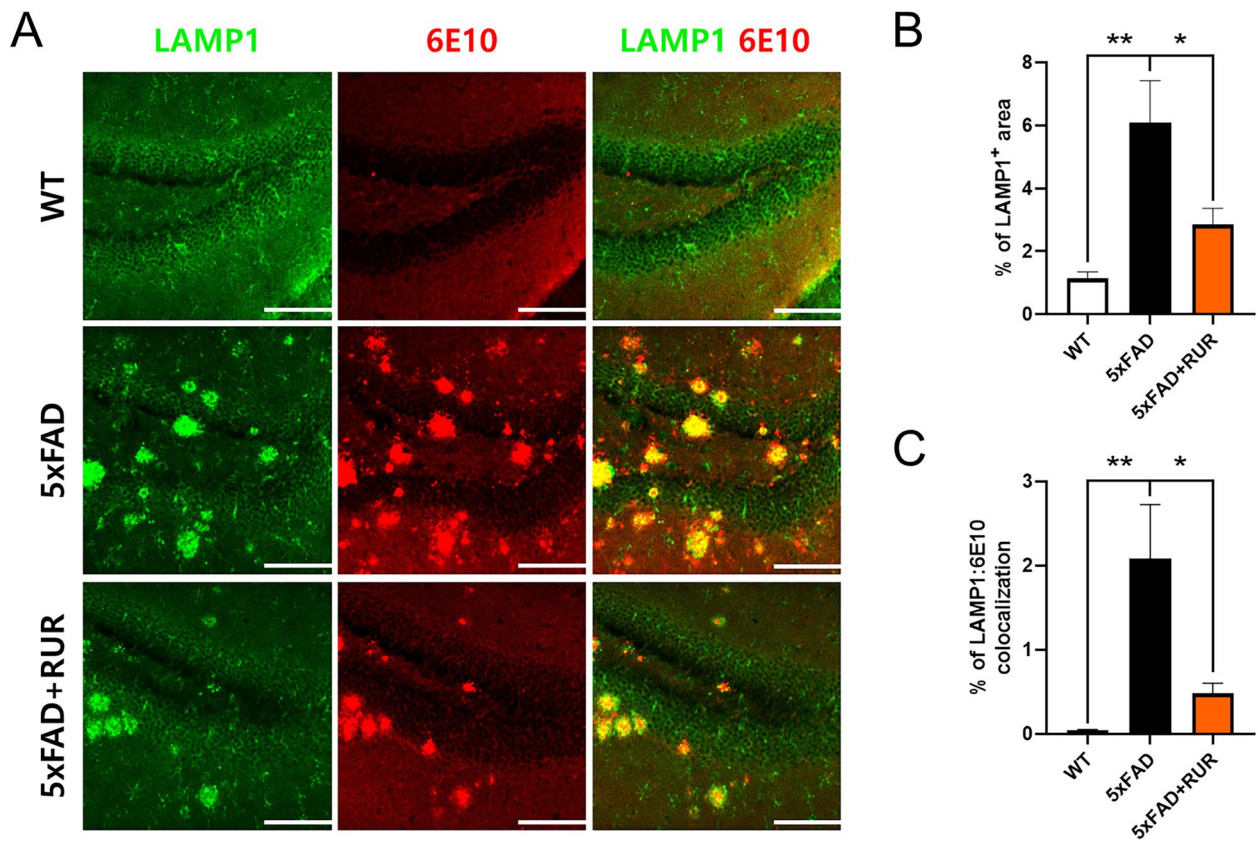


Fig. 4 Effect of RUR administration on the accumulation of DNIs in the hippocampus. Representative photomicrographs of LAMP1 (green) and 6E10 (red) immunopositive areas in the hippocampus are shown ($n=5-6$ per group) (A). The quantification of the LAMP1-positive area was measured by ImageJ (B). The percentage of colocalization (LAMP1:6E10) was measured using a colocalization finder from ImageJ (C). The statistical analyses were performed using ANOVA, followed by Dunnett's post hoc test. $**p < 0.01$ and $*p < 0.05$ vs. 5xFAD group. Scale bar = 200 μm . LAMP1 lysosomal-associated membrane protein 1

to WT mice, while RUR administration reduced the ratio in the hippocampus (Fig. 6C, D). To explore whether RUR ameliorated the hyperphosphorylation of tau, we measured the phosphorylation of GSK-3 β . In AD conditions, the activation of GSK-3 β is increased and induces tau hyperphosphorylation [31]. However, the phosphorylation GSK-3 β at the serine 9 by several kinases such as Akt, suppresses GSK-3 β activation [32]. The GSK-3 β phosphorylation at serine 9 was reduced in vehicle-treated 5xFAD group, compared to the vehicle treated WT group, whereas RUR treatment increased the serine 9-phosphorylated form of GSK-3 β . Moreover, RUR administration increased Akt phosphorylation. Taken together, RUR downregulates GSK-3 β activation by the phosphorylation of serine 9 site via Akt activation, and these results suggest that RUR treatment suppresses tau hyperphosphorylation in the hippocampus of 5xFAD mouse (Fig. 6C, D).

Effect of RUR on A β aggregation in vitro

To confirm how RUR directly reduced A β accumulation in the 5xFAD mouse brain, we performed a Th T assay and dot blot after incubating A β peptides with RUR. NDGA, known to inhibit A β aggregation, was used as a positive control [26]. As a result, RUR incubated with A β_{1-42} monomer reduced aggregated A β compared to A β_{1-42} incubated alone (Fig. 7A). Moreover, to identify whether RUR affects A β oligomers, dot blotting was performed using the A11 antibody that reacts with A β oligomer. As a result, RUR incubated with A β_{1-42} monomer showed less A β_{1-42} oligomer aggregation than A β_{1-42} monomer incubated alone (Fig. 7B). Additionally, RUR incubated with A β_{1-42} oligomer eliminated this form of A β (Fig. 7C).

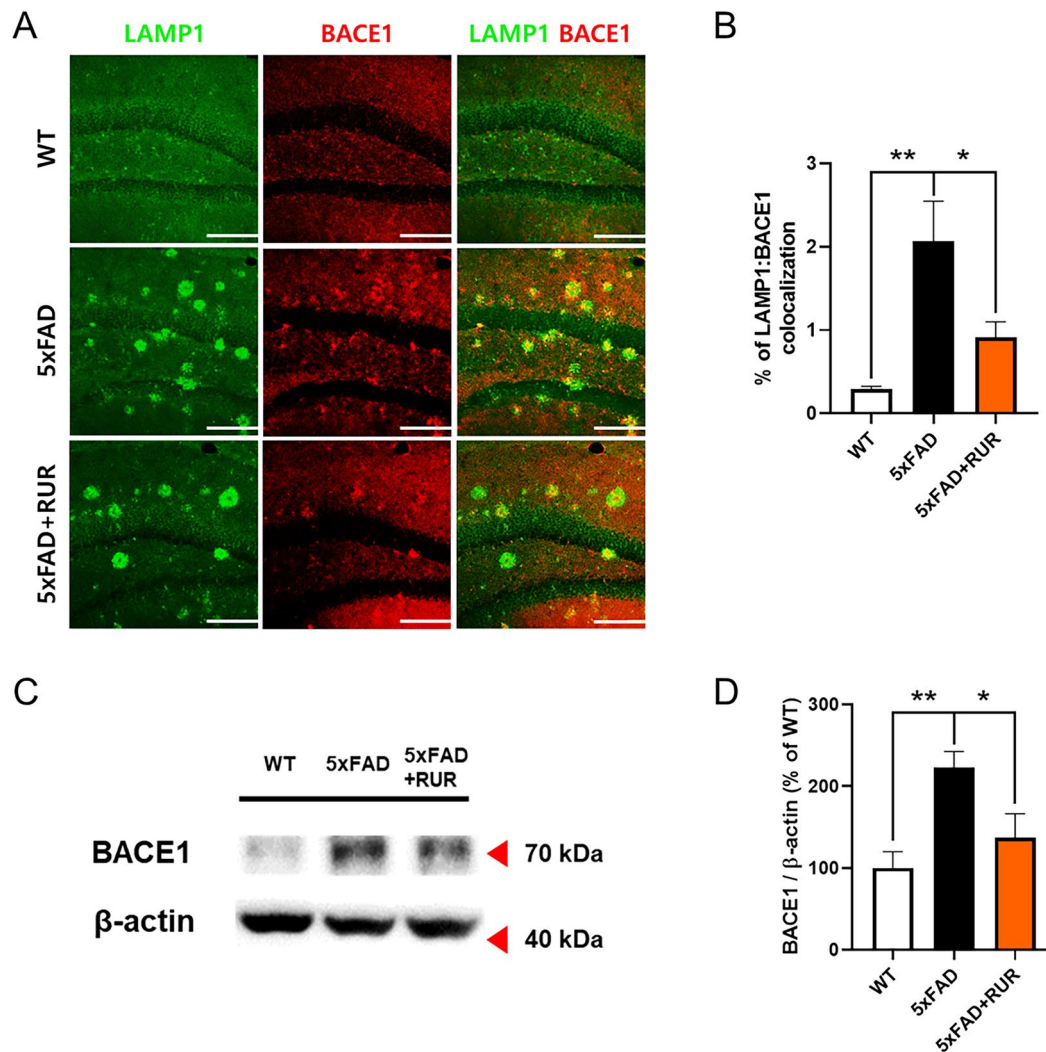


Fig. 5 Effect of RUR administration on the expression of BACE1 within DN in the hippocampus. Representative photomicrographs of LAMP1 (green) and BACE1 (red) immunopositive areas in the hippocampus are shown ($n=5-6$ per group) (A). The percentage of colocalization (LAMP1:BACE1) was measured using a colocalization finder from ImageJ (B). The representative band image (C) and quantification (D) of BACE1 are shown ($n=4-5$ per group). The protein level of BACE1 was normalized to β -actin. The statistical analyses were performed using ANOVA, followed by Dunnett's post hoc test. $**p < 0.01$ and $*p < 0.05$ vs. 5xFAD group. Scale bar = 200 μ m. BACE1 β -site amyloid precursor protein cleaving enzyme 1

Discussion

In this study, we investigated whether RUR treatment alleviated amyloid pathology in human APP and PSEN1 overexpressing transgenic mice. Our results demonstrate that the RUR attenuates memory loss in 5xFAD mice (Fig. 1). Additionally, RUR decreased the accumulation of A β protein including A β monomers, oligomers, and plaques in the brain of 5xFAD mouse (Figs. 2, 3). Additionally, this study showed that RUR alleviated the accumulation of LAMP1 and BACE1 within the DN and tau hyperphosphorylation in the hippocampus (Figs. 4, 5, 6). Lastly, RUR inhibited A β aggregation and eliminated A β oligomers in vitro (Fig. 7).

The amyloid cascade hypothesis posits that A β accumulation in the brain is the primary cause of AD [33]. Under AD conditions, β -secretases induces APP endocytosis and sequentially cleaves APP together with γ -secretase within endosomes to produce monomeric A β , and this peptide is released into the extracellular space [34, 35]. The C-terminal of A β protein induces conformational changes from α -helix to β -sheet [36], leading to the aggregation of A β monomers into β -sheet rich oligomers, protofibrils, and fibrils [37]. In this study, RUR inhibited the further accumulation of A β aggregates in the brain of 5xFAD and suppressed the aggregation of A β peptides in vitro. These results suggest that RUR could

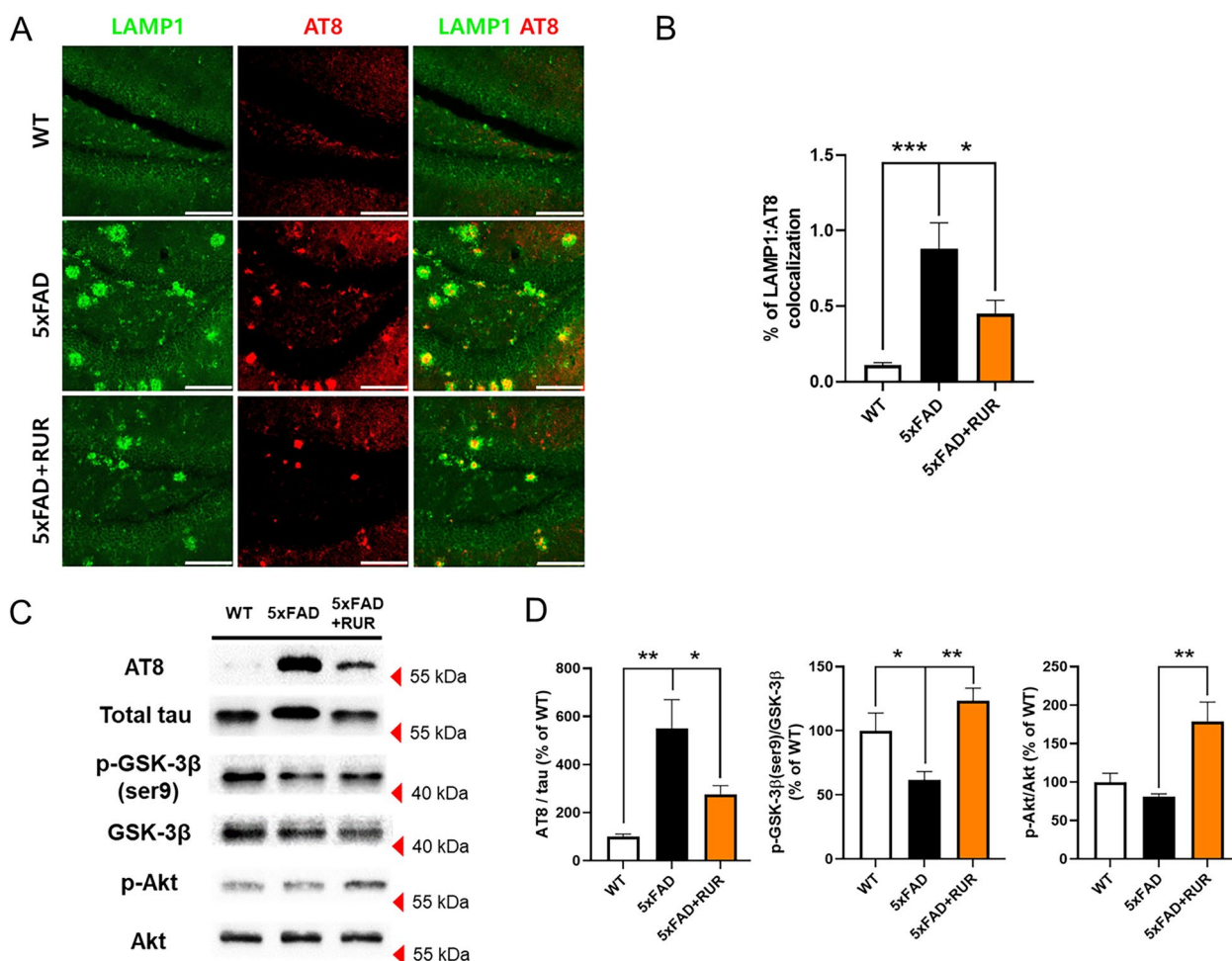


Fig. 6 Effect of RUR administration on the hyperphosphorylation of tau within DN in the hippocampus. Representative photomicrographs of LAMP1 (green) and AT8 (red) immunopositive areas in the hippocampus are shown (n = 5–6 per group) (A). The percentage of colocalization (LAMP1:AT8) was measured using a colocalization finder from ImageJ (B). The representative band (C) and quantification of the AT8 normalized to total tau, p-GSK-3β (ser9) normalized to total GSK-3β, and p-Akt normalized to total Akt (D) are shown (n = 4–5 per group). The statistical analyses were performed using ANOVA, followed by Dunnett’s post hoc test. ***p < 0.001, **p < 0.01 and *p < 0.05 vs. 5xFAD group. Scale bar = 200 μm

directly target Aβ aggregates and protect against their impact on neurotoxicity.

BACE1, a transmembrane protein that plays a role in aspartyl protease activity, is commonly localized in the endosomes of brain neurons [38, 39]. Under healthy conditions, BACE1 is transported through endo-lysosomal organelles and is degraded by the lysosomal pathway [40]. However, as AD progresses, lysosomal dysfunction worsens and BACE1 accumulates in Aβ plaques in the dystrophic axons [41]. Lysosomal dysfunction causes BACE1 and APP to accumulate in immature lysosomes, upregulates β-site cleavage of APP, and increases Aβ production [38, 42]. Moreover, several studies have reported that under stressful conditions caused by pro-inflammatory cytokine, reactive oxygen species, and excitotoxicity,

BACE1 expression increases and Aβ generation is accelerated [43]. Furthermore, Aβ aggregated forms upregulates protein levels of BACE1, indicating the loop of positive feedback [44]. According to several studies, the upregulation of BACE1 in the brain is associated with the development of AD. In this study, RUR treatment reduced the co-staining area of LAMP1 and BACE1, and these results showed that RUR could alleviate BACE1 accumulation within DN around the Aβ deposit.

In the lysosomal degradation pathway, retrograde transport to the cell body is required for lysosomal maturation [45], and mature lysosomes degrade misfolded proteins, such as Aβ, that are delivered by endocytosis, autophagy, and phagocytosis [46]. However, in AD conditions, the excessive accumulation of Aβ causes lysosomal

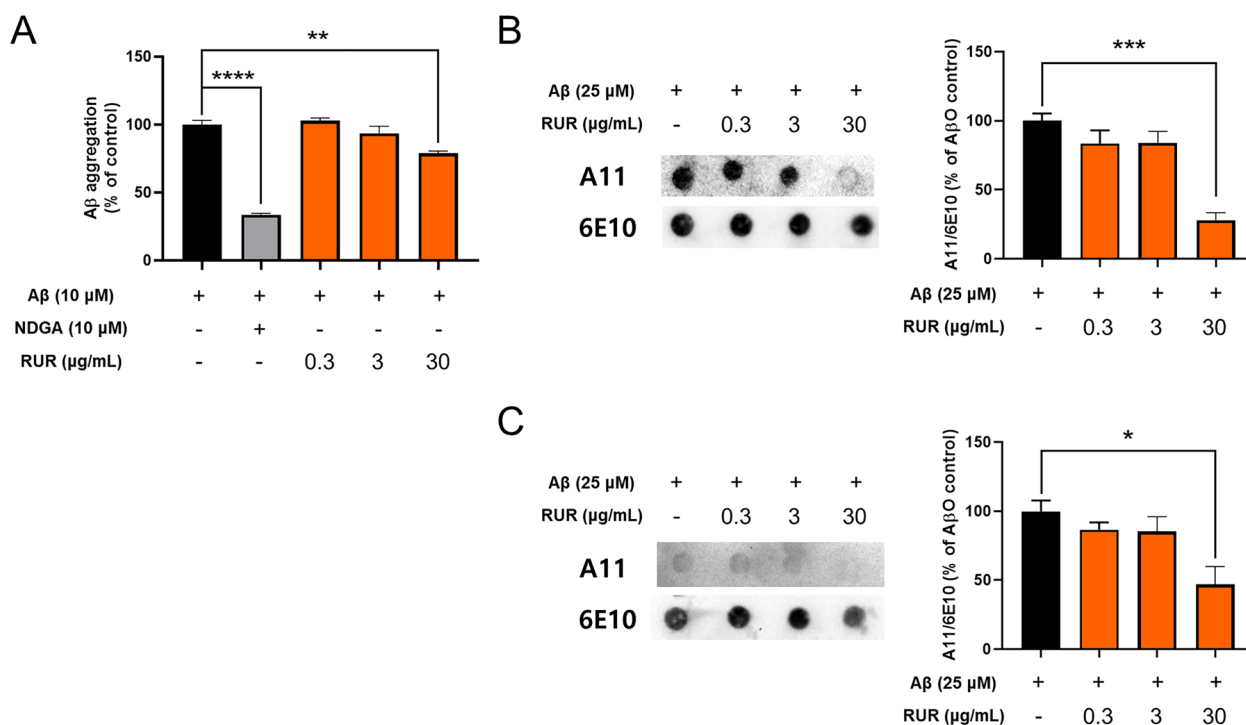


Fig. 7 Effect of RUR on Aβ aggregation in vitro assay. A thioflavin T assay was performed to measure the effects of RUR on Aβ aggregation. Aβ₁₋₄₂ monomer (5 μL of 100 μM) was incubated with PBS or RUR (0.3, 3, or 30 μg/mL) for 48 h at 37 °C (A). Dot blot analysis was performed to measure the effects of RUR on Aβ oligomerization. The Aβ₁₋₄₂ monomer (25 μM) was incubated with PBS or RUR (0.3, 3, or 30 μg/mL) for 24 h at 4 °C (B). Furthermore, the Aβ₁₋₄₂ oligomer (25 μM) was incubated with PBS or RUR (0.3, 3, or 30 μg/mL) for 3 h at 4 °C to measure the effect of RUR on Aβ₁₋₄₂ oligomer degradation (C). Representative bands of A11 and 6E10 were shown (n = 3 per group). The quantification of the A11 band were normalized to the 6E10 band in dot blot analysis. The statistical analyses were performed using ANOVA, followed by Dunnett’s post hoc test. ****p < 0.0001, ***p < 0.001, **p < 0.01, *p < 0.05 vs. Aβ only

dysfunction, and these lysosomes accumulate within dystrophic axons adjacent to the Aβ burden [47]. Therefore, the intracellular transport of lysosomes to the cell body is disrupted by focal axonal swelling [48], resulting in abnormal lysosomal proteolysis, leading to the generation of DNs and lysosomal dysfunction [49]. Additionally, DNs contribute to the accumulation of Aβ plaques, which in turn leads to memory loss, cognitive impairment, neurodegeneration, and synaptic loss [16, 50]. Furthermore, recent studies have reported that mutations in APP and PSEN1 induce lysosomal dysfunction, disrupt axonal transport of lysosomes, and accumulate dysfunctional lysosomes in axons [51]. In this study, we identified that LAMP1-positive lysosomal vesicle accumulate within DNs around Aβ in the hippocampus of the 5xFAD mouse model, which overexpress human APP and PSEN1, and showed that RUR treatment could suppress the accumulation of dysfunctional lysosomes in the 5xFAD mouse.

Furthermore, we evaluated the effect of RUR treatment on tauopathy. Tau is a microtubule-associated protein that stabilizes the cellular cytoskeleton [52]. However, when tau proteins are highly phosphorylated, they

dissociate from the cytoskeleton and accumulate in the brain, consequently inducing tauopathy, which is a pathological feature of AD [53]. In the brains of patients with AD, the levels of phosphorylated tau are 3–4 times higher than in the brains of healthy controls [54]. A previous study reported that the expression of phospho-tau (serine 202/threonine 205) in AD brains could predict the stage of tau pathology and these tau sites are phosphorylated by various kinases, such as GSK-3β and cyclin-dependent kinase 5 [55, 56]. Several studies have been reported that GSK-3β is excessively activated in the brains of AD patients, and the its activation is associated with memory impairment, synaptic loss, and neuroinflammation [57]. Moreover, GSK-3β activation induces Aβ generation and accumulation in the brain [58]. GSK-3β stimulates the mRNA expression of BACE1 thorough NF-κB pathway and induces APP cleavage by BACE1, resulting in Aβ deposits [32]. However, the phosphorylation of GSK-3β at serine 9 by Akt, which is known to play a role in cell survival and apoptosis, inhibits the activation of GSK-3β [59]. The dysfunction of the Akt/GSK-3β signaling pathway leads to excessive activation of GSK-3β, resulting

in accumulation and aggregation of phosphorylated tau in the brain [60]. Several studies have shown that phosphorylated tau accumulates within DNs and blocks the trafficking of organelles in neurons [61, 62]. Moreover, another previous research showed that A β plaque itself can promote or facilitate tau aggregation and accumulation in the AD brain [63]. Abnormal aggregation and accumulation of phosphorylated tau are associated with synaptic loss, neuronal dysfunction, and memory impairment [64, 65]. Therefore, this study evaluated the effects of RUR treatment on tauopathy in the brains of 5xFAD mice by measuring the hyperphosphorylation of tau proteins at the molecular level. RUR treatment decreased the phosphorylation of tau at serine 202 and threonine 205 in the hippocampus of the 5xFAD mouse by regulation of Akt/GSK-3 β signaling pathway. Therefore, our results suggest that RUR may alleviate the pathology of AD caused by tau hyperphosphorylation. However, since we used 5xFAD mice, which do not show neurofibrillary tangles [24], further studies would be required to demonstrate the ameliorative effect of RUR on tauopathy in a different model of AD such as P301S transgenic mice.

Collectively, this study showed that RUR was able to attenuate memory impairment and reduce A β accumulation, DNs formation, and phosphorylated ratio of tau in the hippocampus of 5xFAD mice. RUR treatment could suppress the generation of A β through downregulation of BACE1 within DNs, and directly prevent A β aggregation and degrade A β . Therefore, our results provide obvious evidence that RUR could effectively slow the progression of AD exacerbated by A β pathology, neuritic dystrophy, and hyperphosphorylated tau, and suggest that RUR could be a therapeutic supplement for the treatment of AD.

Abbreviations

6E10	Anti-A β antibody
A11	Anti-oligomer antibody
AD	Alzheimer's disease
APP	Amyloid precursor protein
A β	Amyloid- β
Akt	Protein kinase B
BACE1	β -Site amyloid precursor protein cleaving enzyme 1
CTF	C-terminal fragment
DNs	Dystrophic neurites
ECL	Enhanced chemiluminescence
GAPDH	Glyceraldehyde-3-phosphate dehydrogenase
HRP	Horseradish peroxidase
LAMP1	Lysosomal-associated membrane protein 1
NDGA	Nordihydroguaiaretic acid
PBS	Phosphate-buffered saline
RIPA	Radio-immunoprecipitation assay lysis buffer
PVDF	Polyvinylidene difluoride
RT	Room temperature
RUR	Rhei Undulati Rhizoma
sAPP	Soluble amyloid precursor protein
Th S	Thioflavin S
Th T	Thioflavin T
WT	Wild-type

Supplementary Information

The online version contains supplementary material available at <https://doi.org/10.1186/s13020-024-00966-2>.

Supplementary material 1.

Acknowledgements

The graphical abstract was created in biorender.com.

Author contributions

SL: conceptualization, investigation, methodology, writing—original draft; IGJ: conceptualization, methodology, writing—review and editing; HE: investigation, writing—review and editing; JHK: methodology, validation; YC: investigation, validation; MSO: conceptualization, writing—review and editing, supervision, funding acquisition.

Funding

This research was supported by the Medical Research Center Program through the National Research Foundation of Korea funded by the Ministry of Science and ICT (NRF-2017R1A5A2014768) and a grant of the Korea Health Technology R&D Project through the Korea Health Industry Development Institute (KHIDI), funded by the Ministry of Health & Welfare, Republic of Korea (grand number: HI23C126300).

Availability of data and materials

The datasets analysed during the current study are available from the corresponding author on reasonable request.

Declarations

Ethics approval and consent to participate

All animal studies were approved by the 'Animal Care and Use Guidelines' of Kyung Hee University (approval number: KHUASP(SE)-20-027).

Consent for publication

Not applicable.

Competing interests

The authors declare that they have no known competing financial interests or personal relationships that could have appeared to influence the work reported in this paper.

Author details

¹Department of Biomedical and Pharmaceutical Sciences, Graduate School, Kyung Hee University, 26, Kyungheedaero, Dongdaemun-Gu, Seoul 02447, Republic of Korea. ²Department of Oriental Pharmaceutical Science and Kyung Hee East-West Pharmaceutical Research Institute, College of Pharmacy, Kyung Hee University, 26, Kyungheedaero, Dongdaemun-Gu, Seoul 02447, Republic of Korea. ³Department of Integrated Drug Development and Natural Products, Graduate School, Kyung Hee University, 26, Kyungheedaero, Dongdaemun-Gu, Seoul 02447, Republic of Korea.

Received: 23 February 2024 Accepted: 22 June 2024

Published online: 04 July 2024

References

1. Aisen PS, Cummings J, Jack CR Jr, Morris JC, Sperling R, Frolich L, Jones RW, Dowsett SA, Matthews BR, Raskin J, et al. On the path to 2025: understanding the Alzheimer's disease continuum. *Alzheimers Res Ther*. 2017;9(1):60.
2. Apostolova LG, Green AE, Babakchanian S, Hwang KS, Chou YY, Toga AW, Thompson PM. Hippocampal atrophy and ventricular enlargement in normal aging, mild cognitive impairment (MCI), and Alzheimer disease. *Alzheimer Dis Assoc Disord*. 2012;26(1):17–27.

3. Bloom GS. Amyloid-beta and tau: the trigger and bullet in Alzheimer disease pathogenesis. *JAMA Neurol.* 2014;71(4):505–8.
4. Barage SH, Sonawane KD. Amyloid cascade hypothesis: pathogenesis and therapeutic strategies in Alzheimer's disease. *Neuropeptides.* 2015;52:1–18.
5. Lundgren JL, Ahmed S, Schedin-Weiss S, Gouras GK, Winblad B, Tjernberg LO, Frykman S. ADAM10 and BACE1 are localized to synaptic vesicles. *J Neurochem.* 2015;135(3):606–15.
6. Liu L, Ding L, Rovere M, Wolfe MS, Selkoe DJ. A cellular complex of BACE1 and gamma-secretase sequentially generates Abeta from its full-length precursor. *J Cell Biol.* 2019;218(2):644–63.
7. Zhang X, Fu Z, Meng L, He M, Zhang Z. The early events that initiate beta-amyloid aggregation in Alzheimer's disease. *Front Aging Neurosci.* 2018;10:359.
8. Gandy S. The role of cerebral amyloid beta accumulation in common forms of Alzheimer disease. *J Clin Invest.* 2005;115(5):1121–9.
9. Palop JJ, Mucke L. Amyloid-beta-induced neuronal dysfunction in Alzheimer's disease: from synapses toward neural networks. *Nat Neurosci.* 2010;13(7):812–8.
10. Tarasoff-Conway JM, Carare RO, Osorio RS, Glodzik L, Butler T, Fieremans E, Axel L, Rusinek H, Nicholson C, Zlokovic BV, et al. Clearance systems in the brain—implications for Alzheimer disease. *Nat Rev Neurol.* 2015;11(8):457–70.
11. Tjelle TE, Brech A, Juvet LK, Griffiths G, Berg T. Isolation and characterization of early endosomes, late endosomes and terminal lysosomes: their role in protein degradation. *J Cell Sci.* 1996;109(Pt 12):2905–14.
12. Settembre C, Fraldi A, Medina DL, Ballabio A. Signals from the lysosome: a control centre for cellular clearance and energy metabolism. *Nat Rev Mol Cell Biol.* 2013;14(5):283–96.
13. Whyte LS, Lau AA, Hemsley KM, Hopwood JJ, Sargeant TJ. Endo-lysosomal and autophagic dysfunction: a driving factor in Alzheimer's disease? *J Neurochem.* 2017;140(5):703–17.
14. Sharoar MG, Hu X, Ma XM, Zhu X, Yan R. Sequential formation of different layers of dystrophic neurites in Alzheimer's brains. *Mol Psychiatry.* 2019;24(9):1369–82.
15. Li T, Braunstein KE, Zhang J, Lau A, Sibener L, Deeble C, Wong PC. The neuritic plaque facilitates pathological conversion of tau in an Alzheimer's disease mouse model. *Nat Commun.* 2016;7:12082.
16. Sadleir KR, Kandalepas PC, Buggia-Prevot V, Nicholson DA, Thinakaran G, Vassar R. Presynaptic dystrophic neurites surrounding amyloid plaques are sites of microtubule disruption, BACE1 elevation, and increased Abeta generation in Alzheimer's disease. *Acta Neuropathol.* 2016;132(2):235–56.
17. Brenda RP, Bacsikai BJ, Cirrito JR, Simmons KA, Skoch JM, Klunk WE, Mathis CA, Bales KR, Paul SM, Hyman BT, et al. Anti-Abeta antibody treatment promotes the rapid recovery of amyloid-associated neuritic dystrophy in PDAPP transgenic mice. *J Clin Invest.* 2005;115(2):428–33.
18. Matsuda H, Tewtrakul S, Morikawa T, Yoshikawa M. Anti-allergic activity of stilbenes from Korean rhubarb (*Rheum undulatum* L.): structure requirements for inhibition of antigen-induced degranulation and their effects on the release of TNF-alpha and IL-4 in RBL-2H3 cells. *Bioorg Med Chem.* 2004;12(18):4871–6.
19. Hwang DS, Gu PS, Kim N, Jang YP, Oh MS. Effects of Rhei Undulati Rhizoma on lipopolysaccharide-induced neuroinflammation in vitro and in vivo. *Environ Toxicol.* 2018;33(1):23–31.
20. Burgess EJ. Insulin-like growth factor 1: a valid nutritional indicator during parenteral feeding of patients suffering an acute phase response. *Ann Clin Biochem.* 1992;29(Pt 2):137–44.
21. Jargalsaikhan G, Wu JY, Chen YC, Yang LL, Wu MS. Comparison of the phytochemical properties, antioxidant activity and cytotoxic effect on HepG2 cells in Mongolian and Taiwanese Rhubarb species. *Molecules.* 2021;26(5):1217.
22. Misiti F, Sampaiolese B, Mezzogori D, Orsini F, Pezzotti M, Giardina B, Clementi ME. Protective effect of rhubarb derivatives on amyloid beta (1–42) peptide-induced apoptosis in IMR-32 cells: a case of nutrigenomic. *Brain Res Bull.* 2006;71(1–3):29–36.
23. Xie C, Zhuang XX, Niu Z, Ai R, Lautrup S, Zheng S, Jiang Y, Han R, Gupta TS, Cao S, et al. Amelioration of Alzheimer's disease pathology by mitophagy inducers identified via machine learning and a cross-species workflow. *Nat Biomed Eng.* 2022;6(1):76–93.
24. Oakley H, Cole SL, Logan S, Maus E, Shao P, Craft J, Guillozet-Bongaarts A, Ohno M, Disterhoft J, Van Eldik L, et al. Intraneuronal beta-amyloid aggregates, neurodegeneration, and neuron loss in transgenic mice with five familial Alzheimer's disease mutations: potential factors in amyloid plaque formation. *J Neurosci.* 2006;26(40):10129–40.
25. Eo H, Lee S, Kim SH, Ju IG, Huh E, Lim J, Park S, Oh MS. Petasites japonicus leaf extract inhibits Alzheimer's-like pathology through suppression of neuroinflammation. *Food Funct.* 2022;13(20):10811–22.
26. Ju IG, Lee S, Choi JG, Kim N, Huh E, Lee JK, Oh MS. Aerial part of *Houttuynia cordata* reverses memory impairment by regulating amyloid beta accumulation and neuroinflammation in Alzheimer's disease model. *Phytother Res.* 2023;37(7):2854–63.
27. Choi Y, Huh E, Lee S, Kim JH, Park MG, Seo SY, Kim SY, Oh MS. 5-Hydroxytryptophan reduces levodopa-induced dyskinesia via regulating AKT/mTOR/S6K and CREB/DeltaFosB signals in a mouse model of Parkinson's disease. *Biomol Ther (Seoul).* 2023;31(4):402–10.
28. Gallwitz L, Schmidt L, Marques ARA, Tholey A, Cassidy L, Ulku I, Multhaup G, Di Spiezio A, Saftig P. Cathepsin D: analysis of its potential role as an amyloid beta degrading protease. *Neurobiol Dis.* 2022;175:105919.
29. Kraeuter AK, Guest PC, Sarnyai Z. The Y-Maze for assessment of spatial working and reference memory in mice. *Methods Mol Biol.* 2019;1916:105–11.
30. Ju IG, Lee S, Kim SH, Im H, Eo H, Oh MS. Trichosanthis semen exerts neuroprotective effects in Alzheimer's disease models by inhibiting amyloid-beta accumulation and regulating the Akt and ERK signaling pathways. *J Alzheimers Dis.* 2024;98(1):119–31.
31. Leroy K, Yilmaz Z, Brion JP. Increased level of active GSK-3beta in Alzheimer's disease and accumulation in argyrophilic grains and in neurones at different stages of neurofibrillary degeneration. *Neuropathol Appl Neurobiol.* 2007;33(1):43–55.
32. Lauretti E, Dincer O, Pratico D. Glycogen synthase kinase-3 signaling in Alzheimer's disease. *Biochim Biophys Acta Mol Cell Res.* 2020;1867(5):118664.
33. Hardy J, Selkoe DJ. The amyloid hypothesis of Alzheimer's disease: progress and problems on the road to therapeutics. *Science.* 2002;297(5580):353–6.
34. Wang M, Jing T, Wang X, Yao D. Beta-secretase/BACE1 promotes APP endocytosis and processing in the endosomes and on cell membrane. *Neurosci Lett.* 2018;685:63–7.
35. Rajendran L, Honsho M, Zahn TR, Keller P, Geiger KD, Verkade P, Simons K. Alzheimer's disease beta-amyloid peptides are released in association with exosomes. *Proc Natl Acad Sci U S A.* 2006;103(30):11172–7.
36. Chen GF, Xu TH, Yan Y, Zhou YR, Jiang Y, Melcher K, Xu HE. Amyloid beta: structure, biology and structure-based therapeutic development. *Acta Pharmacol Sin.* 2017;38(9):1205–35.
37. Mirza Z, Pillai VG, Kamal MA. Protein interactions between the C-terminus of Abeta-peptide and phospholipase A2—a structure biology based approach to identify novel Alzheimer's therapeutics. *CNS Neurol Disord Drug Targets.* 2014;13(7):1224–31.
38. Zhao J, Fu Y, Yasvoina M, Shao P, Hitt B, O'Connor T, Logan S, Maus E, Citron M, Berry R, et al. Beta-site amyloid precursor protein cleaving enzyme 1 levels become elevated in neurons around amyloid plaques: implications for Alzheimer's disease pathogenesis. *J Neurosci.* 2007;27(14):3639–49.
39. Vassar R, Bennett BD, Babu-Khan S, Kahn S, Mendiaz EA, Denis P, Teplow DB, Ross S, Amarante P, Loeloff R, et al. Beta-secretase cleavage of Alzheimer's amyloid precursor protein by the transmembrane aspartic protease BACE. *Science.* 1999;286(5440):735–41.
40. Koh YH, von Arnim CA, Hyman BT, Tanzi RE, Tesco G. BACE is degraded via the lysosomal pathway. *J Biol Chem.* 2005;280(37):32499–504.
41. Buggia-Prevot V, Fernandez CG, Riordan S, Vetrivel KS, Roseman J, Waters J, Bindokas VP, Vassar R, Thinakaran G. Axonal BACE1 dynamics and targeting in hippocampal neurons: a role for Rab11 GTPase. *Mol Neurodegener.* 2014;9:1.
42. Kandalepas PC, Sadleir KR, Eimer WA, Zhao J, Nicholson DA, Vassar R. The Alzheimer's beta-secretase BACE1 localizes to normal presynaptic terminals and to dystrophic presynaptic terminals surrounding amyloid plaques. *Acta Neuropathol.* 2013;126(3):329–52.
43. Chami L, Checler F. BACE1 is at the crossroad of a toxic vicious cycle involving cellular stress and beta-amyloid production in Alzheimer's disease. *Mol Neurodegener.* 2012;7:52.
44. Tamagno E, Bardini P, Guglielmotto M, Danni O, Tabaton M. The various aggregation states of beta-amyloid 1–42 mediate different effects on

- oxidative stress, neurodegeneration, and BACE-1 expression. *Free Radic Biol Med.* 2006;41(2):202–12.
45. Tammineni P, Ye X, Feng T, Aikal D, Cai Q. Impaired retrograde transport of axonal autophagosomes contributes to autophagic stress in Alzheimer's disease neurons. *Elife.* 2017;6:e21776.
 46. Pu J, Guardia CM, Keren-Kaplan T, Bonifacino JS. Mechanisms and functions of lysosome positioning. *J Cell Sci.* 2016;129(23):4329–39.
 47. Gowrishankar S, Yuan P, Wu Y, Schrag M, Paradise S, Grutzendler J, De Camilli P, Ferguson SM. Massive accumulation of luminal protease-deficient axonal lysosomes at Alzheimer's disease amyloid plaques. *Proc Natl Acad Sci U S A.* 2015;112(28):E3699–3708.
 48. Wu YT, Gilpin K, Adnan A. Effects of focal axonal swelling level on the action potential signal transmission. *J Comput Neurosci.* 2020;48(3):253–63.
 49. Shi YB, Tu T, Jiang J, Zhang QL, Ai JQ, Pan A, Manavis J, Tu E, Yan XX. Early dendritic dystrophy in human brains with primary age-related tauopathy. *Front Aging Neurosci.* 2020;12:596894.
 50. Peters F, Salihoglu H, Rodrigues E, Herzog E, Blume T, Filser S, Dorostkar M, Shimshek DR, Brose N, Neumann U, et al. BACE1 inhibition more effectively suppresses initiation than progression of beta-amyloid pathology. *Acta Neuropathol.* 2018;135(5):695–710.
 51. Hung COY, Livesey FJ. Altered gamma-secretase processing of APP disrupts lysosome and autophagosome function in monogenic Alzheimer's disease. *Cell Rep.* 2018;25(13):3647–60.
 52. Kadavath H, Hofele RV, Biernat J, Kumar S, Tepper K, Urlaub H, Mandelkow E, Zweckstetter M. Tau stabilizes microtubules by binding at the interface between tubulin heterodimers. *Proc Natl Acad Sci U S A.* 2015;112(24):7501–6.
 53. Spillantini MG, Goedert M. Tau pathology and neurodegeneration. *Lancet Neurol.* 2013;12(6):609–22.
 54. Kopke E, Tung YC, Shaikh S, Alonso AC, Iqbal K, Grundke-Iqbal I. Microtubule-associated protein tau. Abnormal phosphorylation of a non-paired helical filament pool in Alzheimer disease. *J Biol Chem.* 1993;268(32):24374–84.
 55. Alafuzoff I, Arzberger T, Al-Sarraj S, Bodi I, Bogdanovic N, Braak H, Bugiani O, Del-Tredici K, Ferrer I, Gelpi E, et al. Staging of neurofibrillary pathology in Alzheimer's disease: a study of the BrainNet Europe Consortium. *Brain Pathol.* 2008;18(4):484–96.
 56. Engmann O, Giese KP. Crosstalk between Cdk5 and GSK3beta: implications for Alzheimer's disease. *Front Mol Neurosci.* 2009;2:2.
 57. Llorens-Martin M, Jurado J, Hernandez F, Avila J. GSK-3beta, a pivotal kinase in Alzheimer disease. *Front Mol Neurosci.* 2014;7:46.
 58. Jope RS, Yuskaitis CJ, Beurel E. Glycogen synthase kinase-3 (GSK3): inflammation, diseases, and therapeutics. *Neurochem Res.* 2007;32(4–5):577–95.
 59. Su HC, Ma CT, Yu BC, Chien YC, Tsai CC, Huang WC, Lin CF, Chuang YH, Young KC, Wang JN, et al. Glycogen synthase kinase-3beta regulates anti-inflammatory property of fluoxetine. *Int Immunopharmacol.* 2012;14(2):150–6.
 60. Lee CW, Lau KF, Miller CC, Shaw PC. Glycogen synthase kinase-3 beta-mediated tau phosphorylation in cultured cell lines. *NeuroReport.* 2003;14(2):257–60.
 61. Dickson TC, King CE, McCormack GH, Vickers JC. Neurochemical diversity of dystrophic neurites in the early and late stages of Alzheimer's disease. *Exp Neurol.* 1999;156(1):100–10.
 62. Stamer K, Vogel R, Thies E, Mandelkow E, Mandelkow EM. Tau blocks traffic of organelles, neurofilaments, and APP vesicles in neurons and enhances oxidative stress. *J Cell Biol.* 2002;156(6):1051–63.
 63. He Z, Guo JL, McBride JD, Narasimhan S, Kim H, Changolkar L, Zhang B, Gathagan RJ, Yue C, Dengler C, et al. Amyloid-beta plaques enhance Alzheimer's brain tau-seeded pathologies by facilitating neuritic plaque tau aggregation. *Nat Med.* 2018;24(1):29–38.
 64. Drummond E, Pires G, MacMurray C, Askenazi M, Nayak S, Bourdon M, Safar J, Ueberheide B, Wisniewski T. Phosphorylated tau interactome in the human Alzheimer's disease brain. *Brain.* 2020;143(9):2803–17.
 65. Biundo F, Del Prete D, Zhang H, Arancio O, D'Adamio L. A role for tau in learning, memory and synaptic plasticity. *Sci Rep.* 2018;8(1):3184.

Publisher's Note

Springer Nature remains neutral with regard to jurisdictional claims in published maps and institutional affiliations.